

Research Report

Characterization of Rho-GDI γ and Rho-GDI α mRNA in the developing and mature brain with an analysis of mice with targeted deletions of Rho-GDI γ

Russell J. Ferland^{a,1}, Xiaoyu Li^{b,1}, Janet E. Buhlmann^b, Xia Bu^b,
Christopher A. Walsh^{a,*}, Bing Lim^{b,*}

^aDepartment of Neurology, Beth Israel Deaconess Medical Center, Howard Hughes Medical Institute, Harvard Medical School, NRB 266, 77 Avenue Louis Pasteur, Boston, MA 02115, USA

^bDepartment of Medicine, Division of Cancer Biology, Beth Israel Deaconess Medical Center, Harvard Medical School, Harvard Institutes of Medicine, 77 Avenue Louis Pasteur, Boston, MA 02115, USA

Accepted 28 April 2005
Available online 27 July 2005

Abstract

Rho-GDIs are a family of Rho GDP-dissociation inhibitors that are critical in modulating the activity of the small GTPases, Cdc42 and RhoA. Two Rho-GDI isoforms are expressed in the brain, Rho-GDI γ and Rho-GDI α . Here, we describe the expression of both of these isoforms in the developing and mature brain. The mRNA expression patterns of Rho-GDI γ and Rho-GDI α were almost identical in the brain with expression in the developing and mature cerebral cortex, striatum, and hippocampus. In addition, we generated mice with targeted deletions of Rho-GDI γ that are viable and fertile and have no obvious phenotypic abnormalities. Mutant brains looked histologically normal and demonstrated normal patterns of dendritogenesis and neuronal layering as determined by Golgi staining. Mutant mice had normal sleep/wake patterns and sleep EEGs and showed normal hippocampal-dependent learning as assayed by the Morris water maze task. Based on the co-expression of Rho-GDI α and Rho-GDI γ in identical populations of cells in the brain, the lack of phenotype caused by targeted deletion of Rho-GDI γ may not be surprising given that Rho-GDI α may compensate for the loss of Rho-GDI γ . Whether deletion of both Rho-GDI α and Rho-GDI γ , thereby eliminating all GDI activity in the brain, would produce an observable phenotype remains to be determined.

© 2005 Elsevier B.V. All rights reserved.

Theme: Developmental and regeneration

Topic: Developmental genetics

Keywords: Development; GDI; Cortex; Hippocampus; Learning; Knockout

1. Introduction

In response to extracellular signals, the actin cytoskeleton reorganizes and forms well-defined structures that are necessary for proper cell morphology, growth, proliferation, differentiation, motility, and adhesion [5,12,14,17]. The exact mechanisms by which actin reorganizes remain unknown. Three key molecules that control cytoskeletal dynamics are the small GTPase molecules, Rho, Cdc42, and Rac [5,12,14,17]. GTPases cycle between the GDP-bound inactive state and the GTP-bound active state. Rho-GDIs preferentially bind to the GDP-bound form of Cdc42 and

* Corresponding authors. C.A. Walsh is to be contacted at Department of Neurology, Beth Israel Deaconess Medical Center, Howard Hughes Medical Institute, Harvard Medical School, NRB 266, 77 Avenue Louis Pasteur, Boston, MA 02115, USA. Fax: +1 617 667 0815. B. Lim, Department of Medicine, Division of Cancer Biology, Beth Israel Deaconess Medical Center, Harvard Medical School, Harvard Institutes of Medicine, 77 Avenue Louis Pasteur, Boston, MA 02115, USA. Fax: +1 617 667 3299.

E-mail addresses: cwalsh@bidmc.harvard.edu (C.A. Walsh), blim@bidmc.harvard.edu (B. Lim).

¹ These authors contributed equally to the project.

Rac, thereby preventing both the spontaneous and catalyzed release of the GDP by the guanine nucleotide exchange factors. As a result, Rho-GDIs maintain Cdc42 and Rac in the inactive state. Thus, Rho-GDIs are critical modulators that control the molecules necessary for proper actin-cytoskeletal dynamics.

Neurons have varied cellular phenotypes and complex cytoskeletal networks. Cytoskeletal dynamics are critical modulators of neuronal outgrowth and elaboration of dendritic trees and dendritic spines, as well as axonal morphologies [10,16,22,23]. In fact, previous studies have demonstrated the importance of Rho, Rac, and Cdc42 in dendritic and axonal growth as well as in synaptic plasticity [13,16,23]. Moreover, dendritic abnormalities, such as anomalies in dendritic branches and/or spines, are the most consistent neuroanatomical correlate with mental retardation [13]. However, studies are only beginning to address the roles of cytoskeletal genes in mental retardation. Interestingly, PAK3 and oligophrenin, proteins involved in Rho-GTPase signaling, have been directly linked to mental retardation [2,9,13].

To date, there have been only two Rho-GDIs that are expressed in the developing and mature brain, Rho-GDI α and Rho-GDI γ [1,8]. Since Rho-GDIs are critical modulators of the Cdc42 and Rac pathways, it is reasonable to suppose that these molecules also may be critical modulators of cytoskeletal dynamics and thereby possibly affect synaptic plasticity. To that end, we examined the expression patterns of Rho-GDI γ and Rho-GDI α in the developing and mature brain. Furthermore, we generated mice with a targeted disruption of the Rho-GDI γ gene and examined these mice for abnormalities in brain development and cellular morphology in addition to tests of general neurological function. We find that Rho-GDI γ and Rho-GDI α have extensively overlapping patterns of expression in the brain and that a targeted disruption of Rho-GDI γ produces no clear abnormality in brain development or function. These data suggest that Rho-GDI γ alone is not essential to brain development, perhaps because of a compensatory role by Rho-GDI α .

2. Materials and methods

2.1. Animals and histological procedures

For the characterization of the expression patterns of Rho-GDI α and Rho-GDI γ , wildtype Swiss Webster mice from Taconic (Germantown, NY) were sacrificed at different developmental stages (E12.5, E14.5, E16.5, P0.5, P1.5, P3.5, P5.5, P8.5, P15.5, P22.5, and adult) by overdose with sodium pentobarbital, and the brains were processed for either in situ hybridization (ISH) or for Northern blot analysis. Adult C57/BL6J mice from Jackson Laboratories (Bar Harbor, ME) also were used for ISH studies, with both the Rho-GDI α and Rho-GDI γ probes, to test for strain

differences in expression of these two mRNAs. For ISH, the brains of mice were fast frozen in isopentane which was kept on dry ice and stored at -80°C until processed. For histological analysis of knockout mice, mice were perfused transcardially with 0.01 M phosphate-buffered saline (PBS; pH 7.4) followed by cold 4% paraformaldehyde made in PBS. The perfused brains were removed from the head and post-fixed in 4% paraformaldehyde at 4°C . Brains were subsequently cryoprotected in 30% sucrose made in PBS and cut on a cryostat. All animal use procedures were reviewed and approved by the Harvard Medical School Standing Committee on Animals and were in accordance with the National Institutes of Health *Guide for the Care and Use of Laboratory Animals*.

All brains were sectioned either coronally or sagittally (10–20 μm) in a cryostat and mounted on Superfrost plus microscope slides (Fisher Scientific, Pittsburgh, PA). All slides containing cut brain sections were stored at -80°C (ISH) or -20°C (histology) until processed using standard histological techniques as described in the text below.

2.2. Rho-GDI α and Rho-GDI γ Northern blots

Northern blots were performed as previously described [15] following standard conditions. Fifteen micrograms of mouse total brain RNA from (1) either Rho-GDI γ mutant homozygotes ($-/-$) or littermate controls ($+/+$) or (2) from wildtype mice of different developmental stages were separated on a formaldehyde gel, transferred to a nylon membrane, and probed with either a ^{32}P radio-labeled Rho-GDI γ or Rho-GDI α cDNA probe. After washing in a high stringency, low-salt buffer, membranes were exposed to film.

2.3. Rho-GDI α and Rho-GDI γ in situ hybridization

Non-radioactive in situ hybridization (ISH) was performed using digoxigenin-labeled cRNA probes, as previously described [4,7]. The spatial expression patterns of Rho-GDI γ (NCBI: NM008113) and Rho-GDI α (NCBI: AB055070) mRNAs were assessed in mouse brain. The Rho-GDI γ cDNA was cloned into the *Xho*I sites on the pET-15b vector (Novagen, Madison, WI). The Rho-GDI γ probe was constructed by PCR amplifying nucleotides 32 (from the ATG start site) to 491 (forward primer: 5'-AGCAGCTGTTGGAGCTGCTC-3', reverse primer: 5'-GATGGCCTTGTCCACACGCAG-3') and TOPO-TA cloning the PCR product (460 bp) into the pCR $^{\text{®}}$ 4-TOPO vector (Invitrogen, Carlsbad, CA). The T3/T7 priming sites of the pCR $^{\text{®}}$ 4-TOPO vector were used to generate the sense and antisense probes for Rho-GDI γ as described below in more detail. The Rho-GDI α probe was constructed by PCR amplification of mouse ESTs that comprised either the Rho-GDI α coding region (dbEST Id: 9551276) or the Rho-GDI α 3'-UTR (dbEST ID: 6972980). The Rho-GDI α probe for the coding region was a 592 bp PCR product (forward primer:

5'-CAGAACAGGAACCCACTGCT-3', reverse primer: 5'-TTGATGGTGAGATTCCACTCC-3') which started at nucleotide (nt) position 5 (starting from the ATG start site) through nt position 596. The Rho-GDI α probe for the 3'-UTR was a 590 bp PCR product (forward primer: 5'-AGACTCGTCTTGCCGTCTGT-3', reverse primer: 5'-CCAGATCCAACCTCCAGGAAA-3') which started at nt position 747 (starting from the ATG start site) through nt position 1336. All reverse primers contained T7 promoter sequences (5'-TAATACGACTCACTATAGGG-3') on their 5'-ends in order to drive the transcription of the cRNA antisense probes as described below in more detail. DNA sequencing was performed in order to verify the nucleotide composition of the probes. All primers were chosen using Primer3 [20].

For the in situ hybridization studies, brains were obtained at different developmental time points. All brains were frozen in isopentane on dry ice and kept at -80°C until processed. Frozen sections (10 μm) were cut in a cryostat and placed onto Superfrost plus microscope slides. Sections were fixed, acetylated, and hybridized to each probe at 68°C for three nights (approximate concentration 100 ng/ml). Hybridized probes were visualized using alkaline phosphatase-conjugated anti-DIG Fab fragments (Roche, Indianapolis, IN) and 5-bromo-4-chloro-3-indolyl-phosphate/nitro blue tetrazolium (BCIP/NBT) substrate (Kierkegard and Perry Laboratories, Gaithersburg, MD). Following staining, all sections were rinsed in Tris buffer (100 mM Tris, 150 mM NaCl, 20 mM EDTA, pH 9.5) several times and coverslipped with glycerol gelatin (Sigma, St. Louis, MO). Controls for the in situ experiments consisted of incubating sections in either an identical concentration of the sense probe transcript or with another probe directed against a

different sequence from the same gene in order to determine whether this second probe demonstrated an identical labeling pattern. All brain sections were visualized using a Zeiss Axioskop light microscope (Carl Zeiss, Thornwood, NY) and digitally photographed using a SPOT-RT Slider digital camera (Diagnostic Instruments, Inc., Sterling Heights, MI). Contrast, brightness, and enhancement adjustments were made using Adobe[®] Photoshop[®] 5.5 (Adobe Systems, Seattle, WA).

2.4. Generation of mice with targeted disruption of the Rho-GDI γ gene

Using murine Rho-GDI γ cDNA, several sets of PCR primers were used to test genomic DNA for specific PCR fragments which were verified by sequencing. A PCR primer pair was then used to screen a mouse129/SvJ BAC library (Incyte Genomics, Inc., St. Louis, MO). The BAC clones consist of a pBeloBAC11 backbone, with an average insert size of 120 kb. Several overlapping genomic fragments were subcloned, and using these clones, a fine restriction enzyme map was constructed that included defining exon–intron borders. The entire murine Rho-GDI γ gene was mapped to a single 10.9 kb subcloned fragment (Fig. 1).

The targeting vector was constructed by joining together genomic fragments from the Rho-GDI γ gene. An *Xba*I fragment (4.6 kb) from a genomic region upstream of the first exon was excised and ligated into the *Avr*II site of the 38LoxpNeo vector and served as the 5'-homologous arm. A 4.5 kb *Eco*RI/*Hind*II fragment was excised from a genomic region downstream of the last coding exon and ligated into an *Eco*RI/*Hind*III site 3' to the floxed Neo cassette and

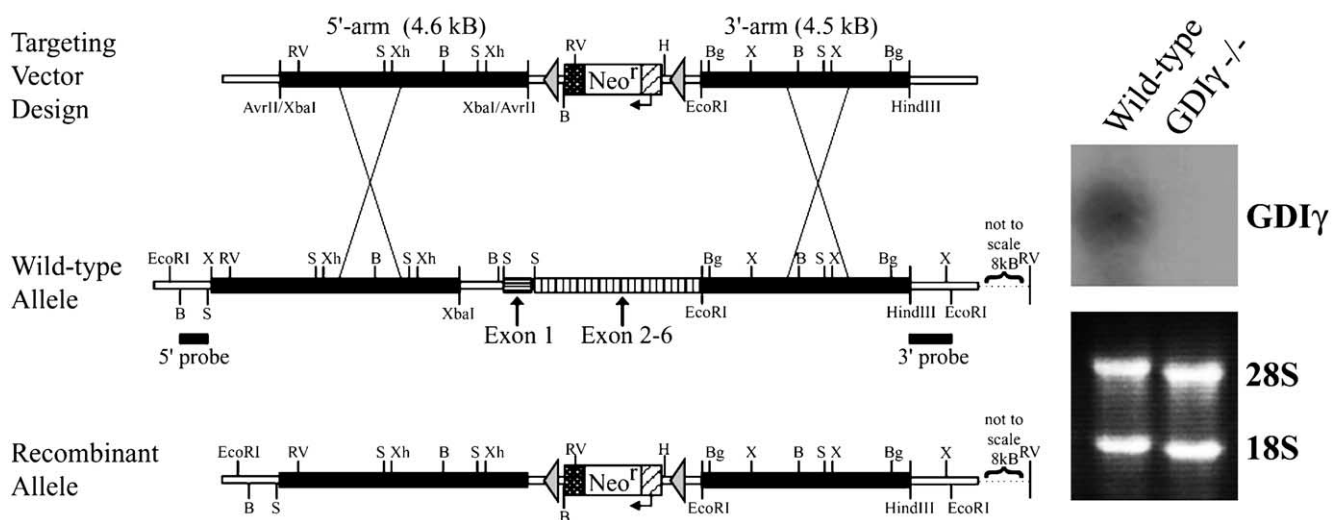


Fig. 1. Construction of targeting vector for Rho-GDI γ deletion showing the main restriction sites within the exons and introns. The wildtype allele is shown with the exons that are replaced by the LoxPNeo cassette in the knockout allele. To screen for homologous recombinant ES clones, a *Bam*HI/*Sac*I fragment was used as the 5'-probe on *Eco*RI digested genomic DNA (wildtype allele: 15.8 kb; recombinant allele: 12.6 kb). Furthermore, an *Eco*RI/*Hind*II fragment was used as the 3'-probe on *Eco*RV digested genomic DNA (wildtype allele: \sim 23 kb; recombinant allele: \sim 18 kb). B = *Bam*HI; Bg = *Bgl*II; RV = *Eco*RV; H = *Hind*III; S = *Sac*I; X = *Xba*I; Xh = *Xho*I. Northern blot demonstrating the expression of Rho-GDI γ total brain RNA in a wildtype mouse and the absence of expression of Rho-GDI γ mRNA in a mouse with a targeted deletion of Rho-GDI γ (GDI γ ^{-/-}).

served as the 3'-homologous arm. A 5.2 kb *XbaI/EcoRI* genomic fragment containing the rest of the Rho-GDI γ coding region was replaced by the floxed neomycin expression cassette upon recombination.

The knockout vector was linearized by a *NotI* restriction enzyme digest before electroporation. Approximately 30 μ g of linearized knockout vector was electroporated into GS1 ES cells (Incyte Genomics, Inc., St. Louis, MO). About 300 clones were isolated after G418 selection. ES clone genomic DNA was extracted for Southern analysis.

For Southern analysis detection of recombination events, a 5'-*BamHI/SacI* fragment and a 3'-*HindIII/EcoRI* fragment (both located outside of the homologous arms) were excised from their respective subclones to use as diagnostic Southern probes. ES clone genomic DNA was digested with *EcoRI* and probed with the 5'-probe predicting a wildtype band of \sim 10 kb and an additional \sim 7 kb band representing the recombinant product following homologous recombination. Similarly, ES cell genomic DNA digested with *EcoRV* and probed with the 3'-probe that was predicted to yield a wildtype band of \sim 23 kb and an additional \sim 18 kb band following homologous recombination.

2.5. Golgi staining

Golgi staining was performed on Rho-GDI γ mutants ($-/-$) and wildtype controls ($+/+$) as previously described [3] with minor modifications. Briefly, all brains were immersed in a solution of 5% potassium dichromate, 5% mercuric chloride, and 4% potassium chromate for 5–6 weeks. The brains were then dehydrated, infiltrated, and embedded in nitrocellulose. The sections were cut under an 80% alcohol drip. Following cutting, the sections were transferred to water and blackened in a 5% solution of sodium carbonate. The sections then were dehydrated in ethanols and cleared in trepeneol. Following a rinse in xylene, the sections were mounted on slides and coverslipped.

2.6. Morris water maze

2.6.1. Group 1

Rho-GDI γ wildtype ($+/+$) and Rho-GDI γ mutants ($-/-$) were trained on a spatial navigation task in the Morris water maze. Two groups of mice were compared to determine their abilities to locate a submerged escape platform in opaque water. Multiple symbols and laboratory equipment were localized throughout the room in which the animals were tested. All animals were tested during the first 8 h of the light cycle. The first groups of mice examined were derived from the first generation of breedings between C57/BL6 wildtype mice and Rho-GDI γ mutants (resulting in F1 generations). These mice were 2–4 months old and were littermate matched. These mice (Rho-GDI γ $+/+$ ($n = 12$) and Rho-GDI γ $-/-$ ($n = 12$)) received four trials per day for four consecutive days using a 4-min inter-trial interval. Between

trials, all animals were dried and placed under a heat lamp in order to maintain body temperature. The location of the platform remained constant in one quadrant of the maze for four consecutive days (Blocks 1–4). However, the starting position for each trial was varied among the four quadrants of the maze and the order differed on each day. For all trials, the dependent measure was recording the latency for the animal to find the platform.

Following the fourth day, the location of the platform was changed to a different quadrant, and the animals were again tested over the course of 4 days (Blocks 5–8). However, for these trials, all mice were tested on a spatial acuity swimming test which examines the ability of the mice to see the symbols that are used to navigate through the maze and also to test for any motoric impairments that the animals might have had in performing the task. This task allows the investigator to determine whether any effects observed in the maze are due to an inability to spatially navigate or are due to motoric or visual impairments. During these trials, the submerged platform was marked by a stick with a large ball on top and placed in a quadrant in which the animals had never had the platform placed during testing. Mice received four trials per day for four consecutive days using a 4-min inter-trial interval and were placed in the maze at four different random locations throughout the maze, and the latency to find the marked platform was recorded.

Following the last marked platform trial, the platform was again hidden, and the location of the platform was changed to a new quadrant. As before, mice received four trials per day as described above (Blocks 9–12), and the latency recorded. During all of these trials, the escape latency was measured with a stopwatch by an investigator who was blind to the genotypes of the mice. The stopwatch was started upon placing the mouse in the maze and stopped when the mouse found the platform.

2.6.2. Group 2

Additional groups of mice were generated from the breeding of F1 generation mutant mice with C57/BL6 wildtype mice. These generations of Rho-GDI γ $+/+$ ($n = 11$) and $-/-$ ($n = 10$) mice, including mice which were heterozygous for the Rho-GDI γ mutation (Rho-GDI γ $+/-$; $n = 6$), were examined also in the Morris water maze. All of these mice were between the ages of 2 and 4 months and were littermate controls. For these experiments, mice received four trials per day (one block) for four consecutive days using a 4-min inter-trial interval. The location of the platform remained constant in one quadrant of the maze for the four consecutive days (Blocks 1–4). However, the starting position for each trial was varied among the four quadrants of the maze, and the order differed on each day.

In addition, on the final day of testing, all mice were exposed to a 180 s probe trial. For the probe trial, the submerged platform was removed from the maze, and the

animals were placed into the water maze. The amount of time spent in each quadrant was recorded as well as the number of times the mice actually swam over the location where the platform was once located.

For all trials with Group 2, the behavior of the animals in the maze was recorded using a CCD camera and the EthoVision[®] software and analysis programs (Noldus Information Technology, Leesburg, VA). The latency to find the submerged platform, the swim velocity, and each swim path was recorded for each individual mouse.

2.7. Data analyses

The data analyses for these experiments consisted of averaging the latencies and velocities (for Group 2 only) of all four trials per day for each animal. A group mean was determined by averaging the trial means for each mouse across the entire group. This resulted in an overall group mean for a block of trials. These block means were plotted for each group and statistically analyzed using repeated measures ANOVA followed by Neuman–Keuls post-hoc analyses and Student's *t* tests. For probe trial analysis, the number of platform crossings was averaged for each group and analyzed using a one-way ANOVA. The percentage of time spent in each quadrant was assessed by repeated measures ANOVA followed by Neuman–Keuls post-hoc analyses and Student's *t* tests.

2.8. Sleep physiology and electroencephalograms (EEG)

Rho-GDI γ mutant mice ($n = 3$) and wildtype controls ($n = 2$) were anesthetized with chloral hydrate and mounted in a small rodent stereotaxic apparatus. A small incision was made in the scalp, and two small holes were made through the skull 1 mm anterior and right to bregma and 1 mm anterior and right to lambda. A screw (Plastics One, Roanoke, VA) was lowered to the surface of the cortex in the most anterior hole and anchored by dental cement. In addition, another EEG screw was anchored to the more posterior hole with dental cement. These EEG screws served as recording electrodes for monitoring brain EEGs. In addition to the EEG electrodes, a silver wire electrode (Plastics One) was inserted and secured in the cervical musculature of the mouse. This electrode was used to monitor electromyograms (EMG). This electrode array allowed us to monitor the sleep/wake patterns of the mice as well as REM and non-REM sleep. All mice were allowed to recover from the surgery and acclimate to the recording chambers for at least 7 days before the start of physiological recordings. After 7 days, all mice had their EEGs and EMGs recorded for 48 h in a temperature–humidity-controlled sound-proof room with a normal 12 h:12 h light:dark cycle (lights on at 07:00). All mice were housed individually. The EEG and EMG signals were recorded as previously described [6]. The proportion of the time the mice were asleep and awake as well as the total

amount of time spent in REM and non-REM sleep was calculated and analyzed as previously described [6].

3. Results

3.1. Rho-GDI γ mRNA expression in the developing and mature brain

Northern blot analysis confirmed the absence of Rho-GDI γ mRNA in the brain of mice with targeted deletions of Rho-GDI γ (Fig. 1). Furthermore, Northern blot analyses of both cerebral cortex (Fig. 2f) and hippocampus (data not shown) demonstrated the expression of Rho-GDI γ mRNA as early as E13. There was a significant, gradual increase in Rho-GDI γ mRNA expression in newborn mice that peaked 8.5 days post partum (Fig. 2f). After P9, Rho-GDI γ mRNA expression began to decrease in cerebral cortex (Fig. 2f) and hippocampus (data not shown), returning to early embryonic levels by P23.

3.2. Rho-GDI γ mRNA expression in the developing and mature brain (in situ hybridization)

To further examine the spatial expression of Rho-GDI γ mRNA, we performed in situ hybridization studies of Rho-GDI γ mRNA. At E14.5, Rho-GDI γ mRNA is expressed throughout the brain at low levels, with the most intense expression occurring in the lateral aspects of the cortical plate (Fig. 2a). This overall low level of expression continues at E16.5, with the highest level of expression in the lateral aspects of the cortical plate as well as in the developing hippocampus (Fig. 2b). In addition, very little expression is observed in the intermediate zone, the region where newly born neurons migrate through in the cortex. By birth (P0.5), Rho-GDI γ mRNA is upregulated with increased expression throughout the developing brain, with the highest expression occurring in the cortical plate (especially the upper half of the cortical plate) (Figs. 2c, c'), the subplate (Figs. 2c, c'), and in the CA1 and CA3 fields of the hippocampus (Fig. 2c''). Very little expression of Rho-GDI γ mRNA is observed in the hippocampal dentate gyrus (Fig. 2c'') and the intermediate zone of the cerebral cortex (Figs. 2c, c'). At P3.5, the cortical plate (especially the middle of the cortical plate) (Fig. 2d') and subplate (Fig. 2d') demonstrate strong expression of Rho-GDI γ mRNA. In addition, hippocampal CA1 and CA3 fields also have high expression, with a low level of expression in the dentate gyrus (Fig. 2d''). By P15.5 (and adult), Rho-GDI γ mRNA is continually expressed in layers 2–6 of the cerebral cortex, with higher levels observed in the layers 5 and 6 of the cortex (Fig. 2e'), as well as in the CA1 and CA3 fields of the hippocampus (Fig. 2e''). No differences were observed in Rho-GDI γ mRNA expression either in adult Swiss Webster mice or in adult C57/BL6J mice, demonstrating that there were no murine strain

Rho-GDI γ mRNA Expression

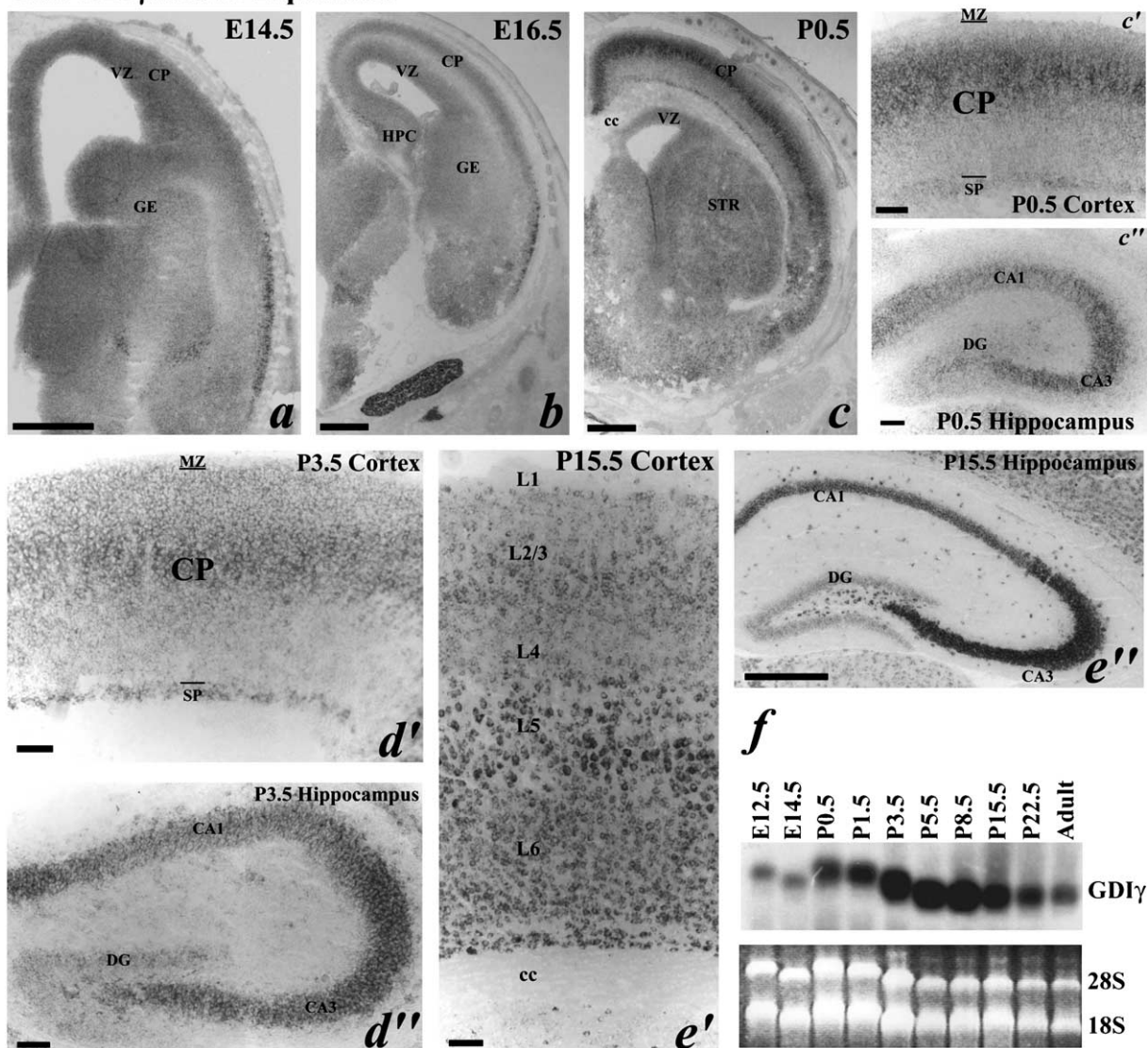


Fig. 2. (a–e). Representative photomicrographs demonstrating the expression patterns of Rho-GDI γ mRNAs in the developing and mature mouse brain. Panels (a) and (b) show low level expression of Rho-GDI γ mRNA throughout the (a) E14.5 and (b) E16.5 brain with higher levels of expression in the lateral cortical plate. (c) At birth (P0.5), Rho-GDI γ mRNA expression is observed throughout the cortical plate and subplate, but especially in the upper half of the cortical plate. In addition, high expression of Rho-GDI γ mRNA also is found in the hippocampal CA1 and CA3 fields. Similar expression patterns for Rho-GDI γ mRNA are observed in the hippocampus at P3.5 (d') and P15.5 (e'). However, the expression of Rho-GDI γ mRNA at P3.5 (d') is highest in the middle of the cortical plate and by P15.5 (e') is expressed throughout cortical layers 2–6. (f) Northern blots showing the expression of Rho-GDI γ total RNA from cerebral cortex of wildtype brain at times ranging from E12.5 to adult (6 weeks old). There is a low level of Rho-GDI γ expression in embryo that increase postnatally until reaching a peak at P8.5 and decreasing to near embryonic levels by P22.5. Ethidium bromide staining of the gel before transfer serves as a loading control. The scale bars in panels (a–c) and (e'') represent 500 μ m. The scale bars in panels (c'), (e'), (d'), (d''), and (e') represent 100 μ m. cc: corpus callosum; CP: cortical plate; DG: dentate gyrus; GE: ganglionic eminences; HPC: hippocampus; L1: cortical layer 1; L2: cortical layer 2; L3: cortical layer 3; L4: cortical layer 4; L5: cortical layer 5; L6: cortical layer 6; MZ: marginal zone; SP: subplate; STR: striatum; VZ: ventricular zone.

differences in Rho-GDI γ mRNA expression (data not shown).

3.3. Targeted disruption of the Rho-GDI γ gene

Our targeting strategy replaced the entire coding region (exons 1–6) of the Rho-GDI γ gene with a neomycin resistance gene cassette, resulting in a complete elimination of the Rho-GDI γ gene. Six ES clones (6/300) were

identified and confirmed for the predicted recombination events on both the 5s- and 3'-homologous arms by diagnostic Southern probing. A neomycin-specific probe indicated a single integration event for these six clones. Karyotyping confirmed a normal male karyotype for these clones. Two clones were used for blastocyst injection experiments. Both clones produced several high percentage male chimeric mice. Two sets of chimeric mice from two ES clones were used to produce +/- offspring. The

phenotypes of the mice produced from both ES lines were identical.

Rho-GDI γ ^{-/-} mice appeared grossly normal. There were no obvious physical abnormalities and in particular no abnormal behavioral traits such as aberrant gait or movement. Female Rho-GDI γ ^{-/-} mice were fertile and bred normally. Hematological and biochemical parameters were all normal (data not shown). In addition, *in situ* hybridization studies using a Rho-GDI γ mRNA probe demonstrated that there was no Rho-GDI γ mRNA expression in our Rho-GDI γ ^{-/-} mutant mice, further confirming our deletion of the Rho-GDI γ gene in our knockout mice (data not shown).

3.4. Rho-GDI γ mutant analysis: gross histology

In order to determine whether Rho-GDI γ mutant mice had any obvious defects in gross neurohistology, we examined cresyl violet stained brain sections from Rho-GDI γ mutant (-/-) mice and wildtype (+/+) mice. No obvious abnormalities were noted upon gross examination of these brain sections (Fig. 3). Mutant mice displayed a normal hippocampus with a compact dentate gyrus and histologically normal CA fields (CA1 and CA3) (Fig. 3). In addition, the hilar region of the mutant animals was indistinguishable from the wildtype controls. Rho-GDI γ mutant mice also displayed a normal six layered cortex that was indistinguishable from the controls (Fig. 3). Lastly, Rho-GDI γ mutant cerebellum also appeared normal as

compared to controls with normal cell layering in the Purkinje and granule cell layers in addition to normal cerebellar foliation (Fig. 3). Overall, there were no gross abnormalities observed in the brains of Rho-GDI γ mutant mice, however, subtle deficits would not be seen at this gross level of examination. Therefore, we explored whether there were any subtle neuroanatomical deficits in the Rho-GDI γ mutant mice by exploring other histological techniques.

Golgi staining, which highlights the extent and complexity of the neuronal dendritic tree, did not reveal any qualitative abnormalities in dendritic arborization (data not shown). Furthermore, immunohistochemical experiments examining cellular markers (i.e. calbindin and MAP2) also did not demonstrate any qualitative differences between Rho-GDI γ mutant and wildtype animals (data not shown).

3.5. Rho-GDI γ mutant analysis: Morris water maze

In order to determine whether the Rho-GDI γ mutant mice had any alterations in learning, we assayed the performance of these animals in the Morris water maze.

3.5.1. Group 1

All mice learned the location of the hidden platform in the Morris water maze task (Fig. 4). On blocks 1–4, there were no differences between the Rho-GDI γ mutant (-/-) mice and the wildtype (+/+) mice in their escape latencies to find the platform ($F_{1,22} = 2.15$; $P > 0.16$), however, there was

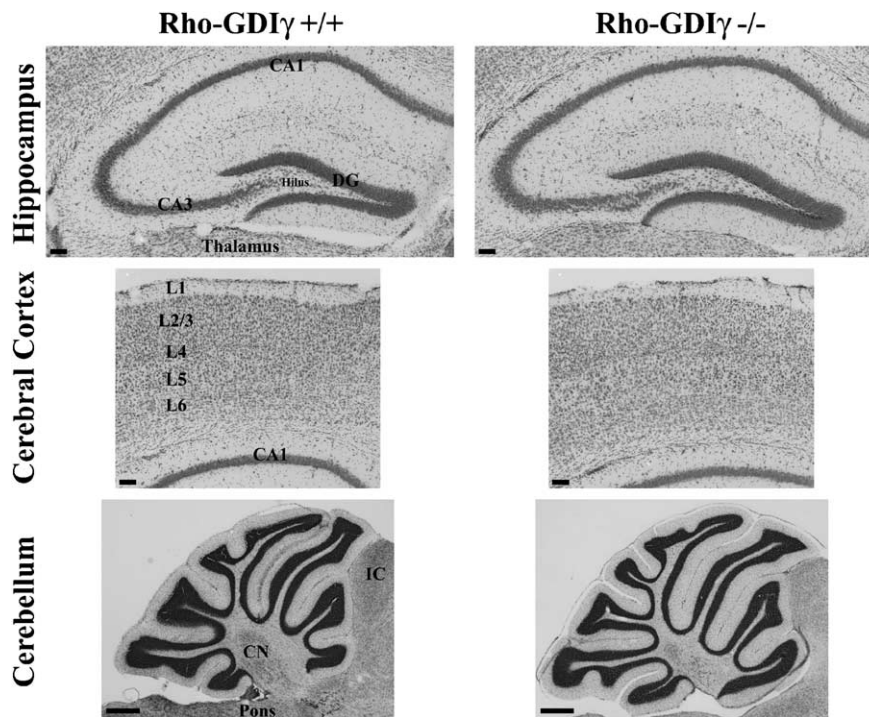


Fig. 3. Histological analysis of Rho-GDI γ ^{-/-} mutant animals as compared to wildtype littermate controls (Rho-GDI γ ^{+/+}). Cresyl violet staining of the hippocampus, cerebral cortex, and cerebellum in Rho-GDI γ ^{-/-} and Rho-GDI γ ^{+/+} mice. There were no neuroanatomical differences observed in comparing the mutant mice versus the wildtype mice. Scale bars represent 100 μ m. CN: deep cerebellar nuclei; DG: dentate gyrus; IC: inferior colliculus; L1: cortical layer 1; L2: cortical layer 2; L3: cortical layer 3; L4: cortical layer 4; L5: cortical layer 5; L6: cortical layer 6.

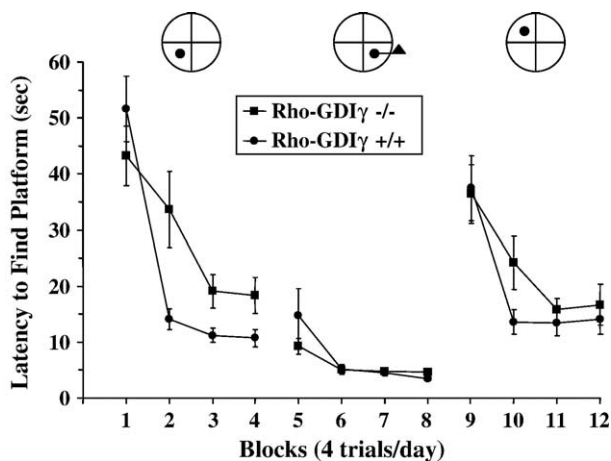


Fig. 4. Plot of the latency for F1 mice (Rho-GDI γ ^{-/-} and Rho-GDI γ ^{+/+}) to find a platform (in seconds) in the Morris water maze across blocks (4 trials/day). Each block represents four trials in which the animal attempts to find the platform each day. The first four blocks demonstrate the ability of the mice to find a hidden platform located in the southwest quadrant of the pool. There were no differences between the two groups in their ability to learn the location of the hidden platform ($F_{1,22} = 2.15$; $P > 0.16$), however, there was a significant interaction effect ($F_{3,66} = 7.49$; $P < 0.0003$). Blocks 5–8 represent the ability of the two groups of animals to find the location of a visible platform placed in a different quadrant (southeast), thereby testing whether there were any differences between the two groups in their physical performance in the maze (i.e. visual acuity, swimming ability, swim speeds, motoric ability, etc.). Importantly, there were no differences between the Rho-GDI γ ^{-/-} and Rho-GDI γ ^{+/+} mice ($F_{1,22} = 0.41$; $P > 0.52$) nor any interaction ($F_{3,66} = 1.63$; $P > 0.19$). Lastly, for blocks 9–12, the platform location was hidden and again moved to a new quadrant (northwest) in order to examine the ability of the mice to reacquire (relearn) the location of the hidden platform. Again, there were no differences between the two groups of animals ($F_{1,22} = 1.63$; $P > 0.21$), and there was no significant interaction ($F_{3,66} = 0.85$; $P > 0.47$).

an effect of learning across blocks in all animals ($F_{3,66} = 53.79$; $P < 0.0000001$), as would be expected in mice that found the submerged platform. Lastly, for blocks 1–4, there was a significant genotype \times block interaction ($F_{3,66} = 7.49$) (Fig. 4).

Blocks 5–8 examined whether there was any motoric, visual, or other impairments that would preclude the ability of the mice to learn in the Morris water maze by analyzing whether there was any difference between Rho-GDI γ mutant mice and wildtype mice in their capacities to find a visible platform. Both Rho-GDI γ mutant and wildtype mice quickly learned the location of the visible platform ($F_{3,66} = 9.89$). More importantly, there were no differences between the two groups in their escape latencies ($F_{1,22} = 0.41$; $P > 0.52$). Moreover, there was no significant genotype \times block interaction ($F_{3,66} = 1.63$; $P > 0.19$) (Fig. 4).

Following the trials on the visible platform task, the location of the platform was again hidden and placed in a different location in the maze (Fig. 4). Similar to performance of the mice in blocks 1–4, there were no significant differences between the Rho-GDI γ mutant and wildtype mice on blocks 9–12 ($F_{1,22} = 1.63$; $P > 0.21$), however,

both groups of mice learned the location of the platform with time ($F_{3,66} = 15.17$) (Fig. 4). Lastly, there was no significant interaction between genotype \times blocks ($F_{3,66} = 0.85$; $P > 0.47$) (Fig. 4).

3.5.2. Group 2

In order to verify our original Morris water data, we examined a second group of mice that were further bred one generation onto a C57/BL6 genetic background. For these experiments, Rho-GDI γ mutant mice ($-/-$), Rho-GDI γ heterozygotic ($+/-$) mice, and wildtype littermate controls ($+/+$) were used. These groups of animals were tested in the Morris water maze using a hidden platform (Fig. 5a). Latencies to find the platform were recorded as well as their swim speeds (cm/s) (Fig. 5b). In addition, these three groups of mice were subjected to a probe trial where the platform was removed and the percentage of time spent in each maze quadrant was recorded (Fig. 5d) along with the frequency of crossing the location of where the platform used to reside (Fig. 5c).

Similar to Group 1, described above, all mice (Rho-GDI γ ^{-/-}, $+/-$, and $+/+$) learned the location of the hidden platform ($F_{3,72} = 62.09$) (Fig. 5a). However, there were no significant differences between the three groups in either their latencies to find the submerged platform ($F_{2,24} = 0.57$; $P > 0.57$) or in any interaction of genotype \times blocks ($F_{6,72} = 1.07$; $P > 0.38$) (Fig. 5a). Moreover, there were no differences in swim velocities between the three groups ($F_{2,24} = 2.05$; $P > 0.15$), suggesting that all groups of mice were performing physically at the same level (Fig. 5b). When mice were analyzed using a probe trial (no platform), there were no differences between the number of times the mice crossed the location of the submerged platform ($F_{2,24} = 0.74$; $P > 0.49$) (Fig. 5c). In addition, the percentage of time spent in each quadrant of the Morris water maze during the probe trial did not differ between the three group of mice ($F_{2,6} < 0.01$; $P > 0.99$) (Fig. 5d). However, there was a significant effect in regard to the amount of time spent in the quadrant which contained the platform on the previous trial (south) in that all three groups of animals spent approximately half of the time in the quadrant where the platform used to reside before this probe trial ($F_{3,6} = 80.63$) (Fig. 5d).

In summary, Rho-GDI γ mutant ($-/-$), heterozygote ($+/-$), and wildtype mice all performed at the same levels in this hippocampal-dependent task of learning.

3.6. Rho-GDI γ mutant analysis: sleep physiology

During routine observations of the Rho-GDI γ mutant ($-/-$) mice in our animal facility, we initially observed that the Rho-GDI γ mutant mice demonstrated altered sleep patterns at a qualitative level. However, since qualitative measures of sleep behavior can be misleading, we sought to determine whether Rho-GDI γ mutant mice had quantitative differences in their sleep patterns, sleep physiology,

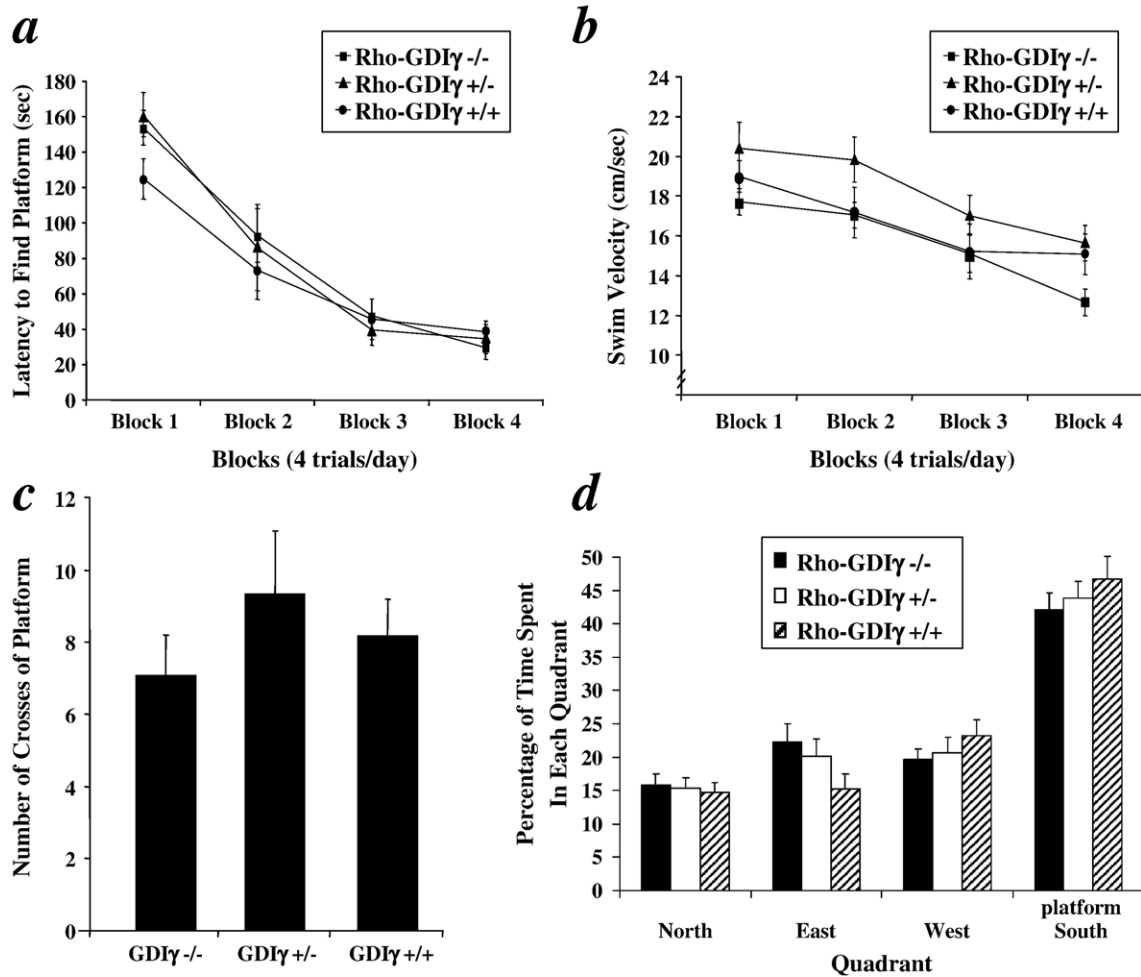


Fig. 5. (a) Plot of the latency for F2 mice (Rho-GDI γ ^{-/-}, +/-, and +/+) to find a platform (in seconds) in the Morris water maze across blocks (4 trials/day). Each block represents four trials in which the animal attempts to find the platform each day. The first four blocks demonstrate the ability of the mice to find a hidden platform located in the south quadrant of the pool. There were no differences between the two groups in their ability to learn the location of the hidden platform ($F_{2,24} = 0.57$; $P > 0.57$) nor any significant interaction effect ($F_{6,72} = 1.07$; $P > 0.38$). (b) Plot of the swim velocities (cm/s) for the three groups of mice across the same trials as in panel (a). There were no differences between the groups in their swim speeds ($F_{2,24} = 2.05$; $P > 0.15$), indicating no gross motor deficits in these mice in their swimming abilities. (c–d) Graph of data from a probe trial in which the platform was removed from the maze and the animals were tested for their skill in remembering the location of the platform. (c) These data represent the frequencies in which the mice actually crossed over the position of where the platform used to reside. There were no significant differences between the three groups of mice (Rho-GDI γ ^{-/-}, +/-, and +/+) in the frequency of crossings ($F_{2,24} = 0.74$; $P > 0.49$). (d) These data demonstrate the percentage of time the mice spent in each quadrant during the probe trial. Again, there were no differences between the Rho-GDI γ ^{-/-}, +/-, and +/+ groups ($F_{2,6} < 0.01$; $P > 0.99$) in the percentage of time spent in each quadrant, however, all three groups of mice spent a significant amount of time in the quadrant that contained the platform (south) as compared to the other quadrants ($F_{3,6} = 80.63$; $P < 0.000001$).

and behavioral states compared to wildtype littermate controls. To that end, we experimentally measured common sleep parameters and physiology (EEG) [6]. Overall, there were no differences between the Rho-GDI γ mutants and controls on measures of total time asleep and total time wake awake, total time in REM and non-REM sleep, and the gross EEG waveforms (data not shown).

3.7. Rho-GDI α mRNA expression in the developing and mature brain (in situ hybridization)

Since there were no apparent behavioral or neuro-anatomical deficits in the Rho-GDI γ mutants, we examined

whether one of the other Rho-GDI isoforms may be expressed in the same regions as Rho-GDI γ and thereby potentially compensating for its loss. To date, there is only one other Rho-GDI that is expressed in the developing and mature brain, Rho-GDI α [1,8]. To examine the expression pattern of this gene, we performed in situ hybridization studies in the developing and mature brain.

Rho-GDI α mRNA is ubiquitously expressed at low levels in the brains of E14.5 mice (Fig. 6a). The highest expression of Rho-GDI α mRNA is in the lateral aspects of the cortical plate. There also appears to be a slightly increased expression of Rho-GDI α mRNA in the ventricular zone (Fig. 6a). At E16.5, Rho-GDI α mRNA is still expressed at relatively low

Rho-GDI α mRNA Expression

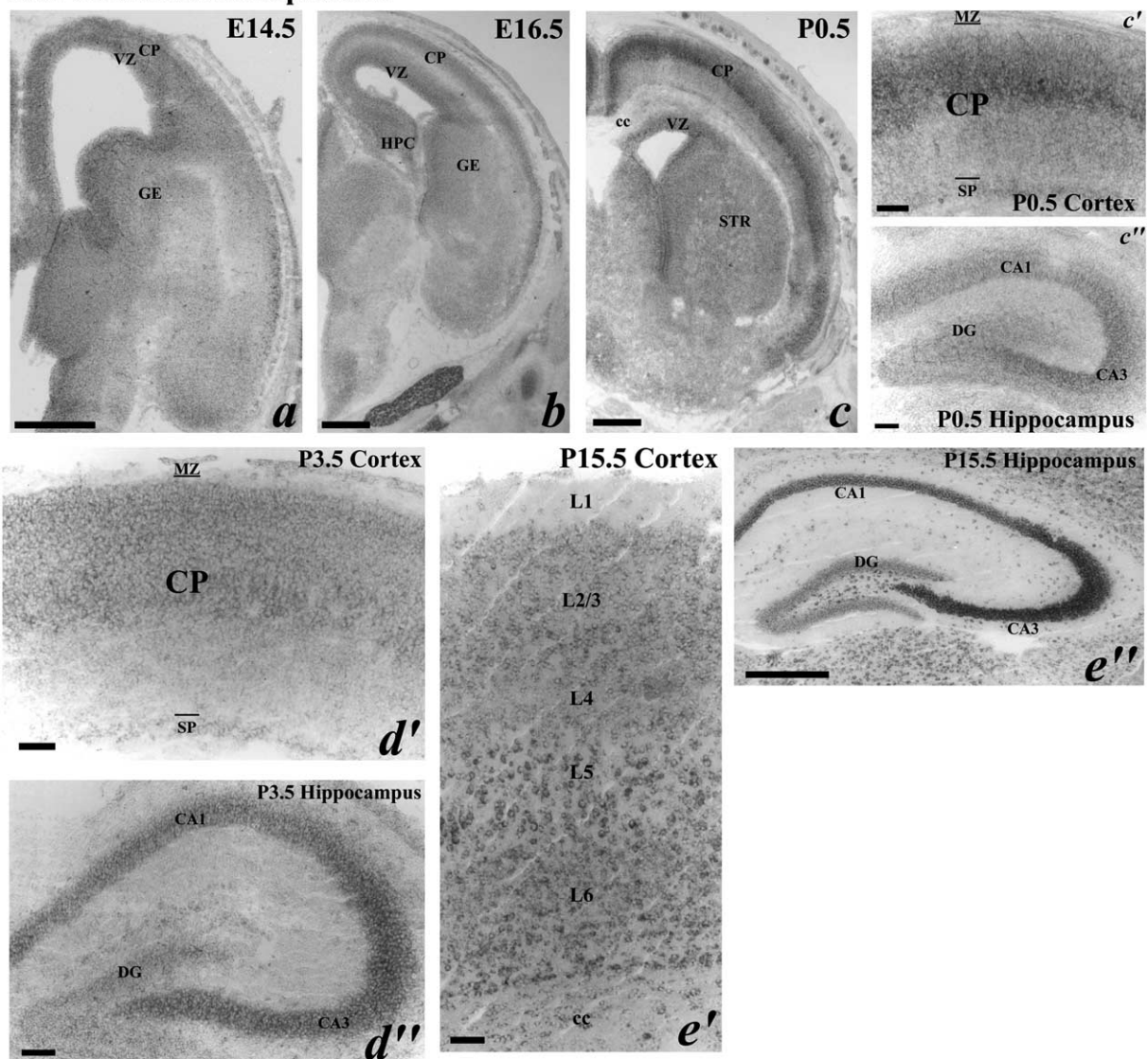


Fig. 6. (a–e) Representative photomicrographs demonstrating the patterns of Rho-GDI α mRNA expression in the mouse brain. Panels (a) and (b) demonstrate low level expression of Rho-GDI α mRNA throughout the (a) E14.5 and (b) E16.5 brain with the highest level of expression in the lateral cortical plate. (c) At birth (P0.5), Rho-GDI α mRNA expression is observed throughout the cortical plate (especially in the upper half) and subplate. Moreover, expression of Rho-GDI α mRNA also is observed in CA1 and CA3 of the hippocampus. At P3.5 (d'') and P15.5 (e''), a similar pattern of expression is observed for Rho-GDI α mRNA as was seen at P0.5. However, the expression of Rho-GDI α mRNA at P3.5 is highest in the middle of the cortical plate (d') and by P15.5 is expressed throughout cortical layers 2–6 (e'). The scale bars in panels (a–c) and (e') represent 500 μ m. The scale bars in panels (c'), (c''), (d'), (d''), and (e'') represent 100 μ m. cc: corpus callosum; CP: cortical plate; DG: dentate gyrus; GE: ganglionic eminences; HPC: hippocampus; L1: cortical layer 1; L2: cortical layer 2; L3: cortical layer 3; L4: cortical layer 4; L5: cortical layer 5; L6: cortical layer 6; MZ: marginal zone; SP: subplate; STR: striatum; VZ: ventricular zone.

levels in the developing brain (Fig. 6b). Cells in the lateral aspects of the cortical plate continue to express Rho-GDI α mRNA at high levels, with a decrease in the expression of Rho-GDI α mRNA in the ventricular zone. Moreover, there is a relative paucity of Rho-GDI α mRNA expression in the intermediate zone of the developing cortex (Fig. 6b). At birth (P0.5), Rho-GDI α mRNA is highly expressed in the cortical plate, especially in the upper half of the cortical plate (Figs. 6c, c'), in the hippocampal CA fields (CA1 and CA3) (Fig. 6c''), and in the subplate (Figs. 6c, c'). Low levels of expression of Rho-GDI α mRNA are observed in the lower

half of the cortical plate (Figs. 6c, c'), the hippocampal dentate gyrus (Fig. 6c''), and the striatum (Fig. 6c). The middle of the cortical plate demonstrates slightly higher expression of Rho-GDI α mRNA at P3.5 (Fig. 6d'), while the subplate (Fig. 6d') and hippocampal CA1 and CA3 fields (Fig. 6d'') continue to express high levels of Rho-GDI α mRNA (very little dentate gyrus expression; Fig. 6d''). Finally, high Rho-GDI α mRNA expression is found in cortical layers 2–6 of the P15.5 brain (and adult), especially in the lower layers (Fig. 6e'). Hippocampal Rho-GDI α mRNA expression is observed throughout the hippocampus

especially in CA1 and CA3 (Fig. 6e''). No differences were observed in Rho-GDI α expression either in adult Swiss Webster mice or in adult C57/BL6J mice, demonstrating that there were no strain differences in its expression (data not shown).

The Rho-GDI α mRNA expression pattern is almost identical to that observed for Rho-GDI γ mRNA expression (Fig. 7). This high concordance in expression pattern may be responsible for the lack of a phenotype in our Rho-GDI γ mutant mice. Northern blot analysis of Rho-GDI α in Rho-GDI γ ($-/-$) mutant mice did not demonstrate any obvious quantitative alterations in the levels of Rho-GDI α mRNA expression in brain, suggesting that there were no compensatory increases in its expression (data not shown). Moreover, in situ hybridization studies in the Rho-GDI γ mutant for Rho-GDI α mRNA expression showed that there were no changes in the spatial distribution or expression of Rho-GDI α mRNA as compared to wildtype mice (Fig. 8). These studies would suggest that any compensatory changes of Rho-GDI α in the Rho-GDI γ mutant background do not occur through either an increase in expression or change in spatial distribution of Rho-GDI α but is simply a result of a redundancy in these two brain specific Rho-GDIs. Future work is needed in order to determine whether Rho-GDI α is compensating for a lack of Rho-GDI γ in our mutant mice through analyses using mice that are null for both Rho-GDI α and Rho-GDI γ .

4. Discussion

Rho-GDI γ and Rho-GDI α demonstrated almost identical patterns of mRNA expression in the brain in the cerebral cortex, striatum, and hippocampus (CA fields). Little mRNA expression was seen in the embryonic ventricular zone or the hippocampal dentate gyrus. Mice with targeted

deletions of Rho-GDI γ are viable and fertile with no obvious abnormalities. The brains of Rho-GDI γ mutants appeared histologically normal, had normal sleep–wake cycles and sleep EEGs, and demonstrated normal hippocampal-dependent learning. However, Rho-GDI α and Rho-GDI γ mRNA expression was virtually indistinguishable in the central nervous system, and the lack of phenotype in mice with targeted-deletions of Rho-GDI γ may have resulted from a compensatory role of Rho-GDI α . Further experiments are in progress to determine whether deletions of both Rho-GDI α and Rho-GDI γ would produce an observable brain or behavioral phenotype.

The Rho-GDI family of proteins (α , β , and γ) is one of three central regulators of the RhoA/Rac/Cdc42 family of small GTPases [25]. Thus far, three Rho-GDIs have been identified. Rho-GDI α was first cloned from brain and was found to be ubiquitously expressed [8]. Rho-GDI β was found to be preferentially expressed in hematopoietic cells [15]. Rho-GDI γ was cloned from a whole embryo library and was found to be expressed at high levels in only 2 tissues, brain and pancreas [1]. The biochemical function of Rho-GDIs has been shown to inhibit the dissociation of GDP from RhoGTPases, in vitro, thereby preventing the exchange for GTP and the activation of RhoGTPases [21]. Interestingly, all three Rho-GDIs are capable of exerting the same inhibitory effect on the same RhoGTPase substrates such as Cdc42 and Rac although with different efficacy [1,15,19]. Therefore, there is a potential redundancy of Rho-GDI function. Rho-GDIs were also thought to be involved in the shuttling of RhoGTPases between membrane and cytoplasmic compartments. Since the RhoA/Rac/Cdc42 family of RhoGTPases are involved in a great diversity of fundamental cellular functions, regulators of their activated functional state would in turn play a central role in modulating the effect of RhoGTPases. One way to reveal the impact and real biological function of GDIs would be to disrupt their

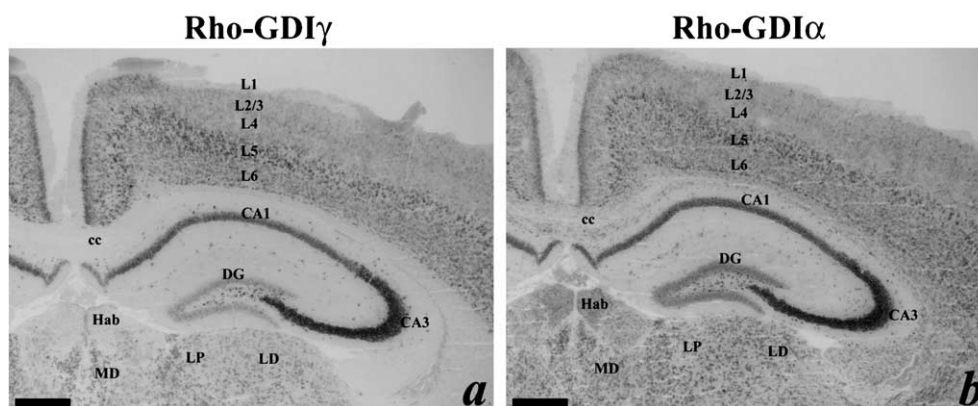


Fig. 7. Representative photomicrographs demonstrating the patterns of Rho-GDI γ (a) and Rho-GDI α (b) mRNA expression in the mouse brain. In situ hybridization studies examining the expression of Rho-GDI γ and Rho-GDI α mRNA indicated virtually identical patterns of expression, suggesting that the lack of a behavioral or neuroanatomical defect in the Rho-GDI γ mutant may be due to a compensation by Rho-GDI α in the mutant. Scale bars represent 500 μ m. cc: corpus callosum; DG: dentate gyrus; Hab: habenular nucleus; L1: cortical layer 1; L2: cortical layer 2; L3: cortical layer 3; L4: cortical layer 4; L5: cortical layer 5; L6: cortical layer 6; LD: lateral–dorsal nucleus of the thalamus; LP: lateral–posterior nucleus of the thalamus; MD: medial–dorsal nucleus of the thalamus.

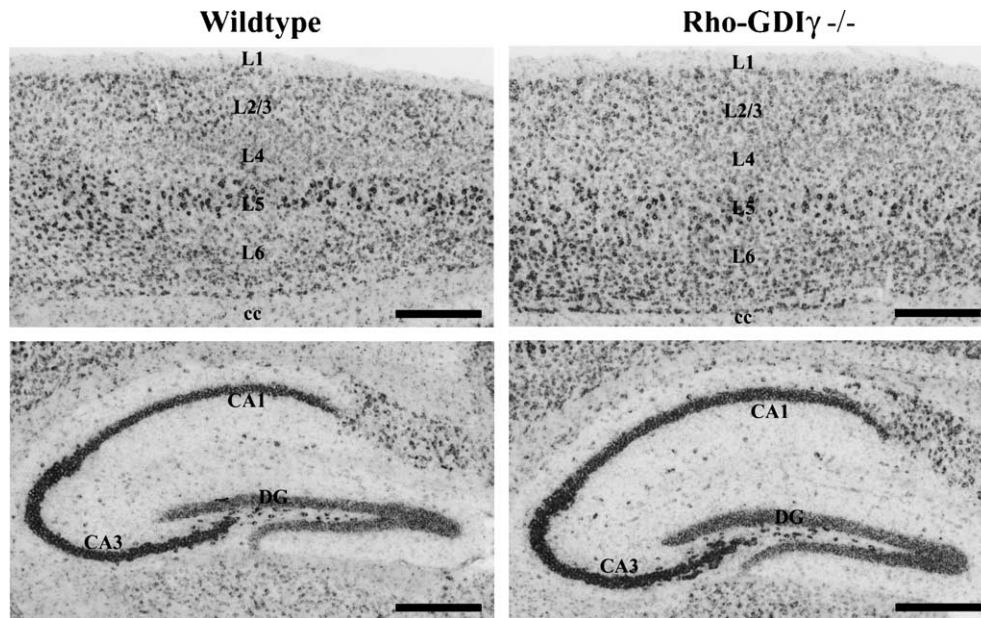


Fig. 8. Representative photomicrographs indicating the patterns of Rho-GDI α mRNA expression in either wildtype or Rho-GDI γ mutant ($-/-$) brain, particularly in the cerebral cortex (upper panels) and hippocampus (lower panels). In situ hybridization studies examining the expression of Rho-GDI α mRNA in wildtype or Rho-GDI γ mutant ($-/-$) brain demonstrated virtually no changes in the spatial or quantitative (i.e. upregulation) levels of Rho-GDI α in comparing both the wildtype and mutant. Since there was no evidence for an upregulation of Rho-GDI α mRNA in the Rho-GDI γ mutant brain, this suggests that the lack of a behavioral or neuroanatomical defect in the Rho-GDI γ mutant may be due to a compensation by Rho-GDI α that is not due to a simple change in the expression of this other brain GDI isoform. Scale bars represent 500 μ m. cc: corpus callosum; DG: dentate gyrus; L1: cortical layer 1; L2: cortical layer 2; L3: cortical layer 3; L4: cortical layer 4; L5: cortical layer 5; L6: cortical layer 6.

function in an organism. Rho-GDI α mutant ($-/-$) mice are born alive, but male animals were found to be sterile, and by 5 to 6 months of age develop an unusual renal sclerosis pathology with animals subsequently dying from renal failure [24]. Rho-GDI β $-/-$ animals are normal with no significant hematopoietic defect except for a mild defect in macrophage superoxide production [11]. The absence of a more dramatic phenotype and biochemical defect in these loss-of-function mutants very likely reflects the redundancy of function between different Rho-GDIs. It is also possible that other Rho-GDIs have not yet been identified that further add to this redundancy.

As mentioned earlier, the RhoA/Rac/Cdc42 pathway that is regulated by Rho-GDIs is a critical modulator of dendritogenesis. Based on our expression data, Rho-GDI γ is widely expressed throughout the brain with the highest levels of expression occurring during the first 2 weeks of life. This increased window of expression is at a time when there is intense elaboration of the dendritic trees of neurons in the developing brain [18]. These data, although correlative, suggest the possibility that Rho-GDI γ may play an important role in the process of dendritogenesis.

Based on this hypothesis and since our expression data demonstrate high levels of Rho-GDI γ mRNA in hippocampus and cortex, we examined whether mice with targeted deletions of Rho-GDI γ had any abnormalities in neuronal morphology or in behavioral processes mediated by mechanisms of dendritogenesis. Thus, we examined whether Rho-GDI γ mutant mice had any deficits as

revealed by histology, sleep physiology, or learning experiments. Our histological analysis of Rho-GDI γ mutant and wildtype mice did not reveal any obvious qualitative differences between these groups of mice in regard to the structure of the brain or in the dendritic morphology of neurons. These results suggest that, if there are subtle defects in the brains of these mutant mice, then standard histological techniques may not be sensitive enough to detect any morphological abnormalities. Therefore, we performed behavioral experiments designed to detect differences between Rho-GDI γ mutant and wildtype mice.

Unfortunately, we were unable to detect any significant differences between Rho-GDI γ mutant and wildtype mice on measures of sleep physiology and learning. Our analysis of sleep patterns and EEGs of Rho-GDI γ mutant and wildtype mice were unable to detect any significant differences in these parameters, suggesting that Rho-GDI γ alone is not directly involved in sleep or in the underlying processes responsible for sleep. Moreover, learning experiments performed on Rho-GDI γ mutant and wildtype mice in the Morris water maze also were unable to detect differences between these two groups of mice. Rho-GDI γ mutants, heterozygotes, and wildtype mice were all able to learn the maze with no significant differences between these groups. Similar to the sleep experiments, our data suggest that Rho-GDI γ alone is not involved in learning or in the neural processes that mediate learning (i.e. synaptic plasticity).

In order to determine why we were unable to detect any brain phenotypes, we examined the expression patterns of

the only other known Rho-GDI that is expressed in the brain, Rho-GDI α . The expression pattern of Rho-GDI α mRNA was virtually identical to that of Rho-GDI γ mRNA. This finding suggests that Rho-GDI α may be compensating for the absence of Rho-GDI γ in our mice with targeted deletions of Rho-GDI γ since there is a redundancy of function between different Rho-GDIs. This interpretation indicates that the reason for not observing any abnormalities in our mutant animals was due to a compensation by Rho-GDI α . However, this compensation is not a result of a simple increase or change in spatial expression of Rho-GDI α mRNA in the Rho-GDI γ mutant mice. Furthermore, as mentioned earlier, Rho-GDI α mutant ($-/-$) mice are not reported to have any brain abnormalities [24], further adding to this dichotomy. In order to address this issue, studies are needed that breed the Rho-GDI α and Rho-GDI γ mutant mice in order to obtain double knockouts for these two genes. These experiments would help elucidate the role that Rho-GDIs are playing in the brain and will help us to understand the role that brain Rho-GDIs play in cognition.

Acknowledgments

This study was supported in part by a training grant from NIH T32 HD07466 (R.J.F.), a Young Investigator Award from Cure Autism Now (R.J.F.), and a NIMH KO1 award (MH071801-01) (R.J.F.). Additional support for this work was provided by grants from NIH RO1 DK47636 (B.L.), RO1 AI54973 (B.L.), and RO1 NS32457 (C.A.W.). C.A.W. is an Investigator in the Howard Hughes Medical Institute.

The authors would like to thank Urs Berger, PhD for assistance in the implementation and performing of in situ hybridization studies. We also would like to thank the Thomas Scammell and Clifford Saper laboratories for the use of their sleep physiology equipment and set-up as well as helpful advice with the implementation, design, and analysis of the experiments. In addition, the authors would like to thank Craig Applegate, PhD for helpful discussions.

References

- [1] C.N. Adra, D. Manor, J.L. Ko, S. Zhu, T. Horiuchi, L. Van Aelst, R.A. Cerione, B. Lim, RhoGDI γ : a GDP-dissociation inhibitor for Rho proteins with preferential expression in brain and pancreas, *Proc. Natl. Acad. Sci. U. S. A.* 94 (1997) 4279–4284.
- [2] K.M. Allen, J.G. Gleeson, S. Bagrodia, M.W. Partington, J.C. MacMillan, R.A. Cerione, J.C. Mulley, C.A. Walsh, PAK3 mutation in nonsyndromic X-linked mental retardation, *Nat. Genet.* 20 (1998) 25–30.
- [3] J. Bancroft, A. Stevens, *Theory and Practice of Histological Techniques*, Churchill-Livingstone, London, 1982.
- [4] U.V. Berger, M.A. Hediger, Differential distribution of the glutamate transporters GLT-1 and GLAST in tanycytes of the third ventricle, *J. Comp. Neurol.* 433 (2001) 101–114.
- [5] K. Carraway, C. Carraway, K. Carraway III, *Signaling and the Cytoskeleton*, Springer, New York, 1998.
- [6] I.V. Estabrooke, M.T. McCarthy, E. Ko, T.C. Chou, R.M. Chemelli, M. Yanagisawa, C.B. Saper, T.E. Scammell, Fos expression in orexin neurons varies with behavioral state, *J. Neurosci.* 21 (2001) 1656–1662.
- [7] R.J. Ferland, T.J. Cherry, P.O. Preware, E.E. Morrisey, C.A. Walsh, Characterization of Foxp2 and Foxp1 mRNA and protein in the developing and mature brain, *J. Comp. Neurol.* 460 (2003) 266–279.
- [8] Y. Fukumoto, K. Kaibuchi, Y. Hori, H. Fujioka, S. Araki, T. Ueda, A. Kikuchi, Y. Takai, Molecular cloning and characterization of a novel type of regulatory protein (GDI) for the rho proteins, ras p21-like small GTP-binding proteins, *Oncogene* 5 (1990) 1321–1328.
- [9] E.E. Govek, S.E. Newey, C.J. Akerman, J.R. Cross, L. Van Der Veken, L. Van Aelst, The X-linked mental retardation protein oligophrenin-1 is required for dendritic spine morphogenesis, *Nat. Neurosci.* 7 (2004) 364–372.
- [10] K.L. Guan, Y. Rao, Signalling mechanisms mediating neuronal responses to guidance cues, *Nat. Rev. Neurosci.* 4 (2003) 941–956.
- [11] J.C. Guillemot, B.A. Kruskal, C.N. Adra, S. Zhu, J.L. Ko, P. Burch, K. Nocka, K. Seetoo, E. Simons, B. Lim, Targeted disruption of guanosine diphosphate-dissociation inhibitor for Rho-related proteins, GDID4: normal hematopoietic differentiation but subtle defect in superoxide production by macrophages derived from in vitro embryonal stem cell differentiation, *Blood* 88 (1996) 2722–2731.
- [12] P. Jeanteur, Cytoskeleton and small G proteins, *Prog. Mol. Subcell Biol.* 22 (1999).
- [13] W.E. Kaufmann, H.W. Moser, Dendritic anomalies in disorders associated with mental retardation, *Cereb. Cortex* 10 (2000) 981–991.
- [14] J. Lackie, G. Dunn, G. Jones, *Cell Behaviour: Control and Mechanisms of Motility*, Portland, London, 1999.
- [15] J.M. Lelias, C.N. Adra, G.M. Wulf, J.C. Guillemot, M. Khagad, D. Caput, B. Lim, cDNA cloning of a human mRNA preferentially expressed in hematopoietic cells and with homology to a GDP-dissociation inhibitor for the rho GTP-binding proteins, *Proc. Natl. Acad. Sci. U. S. A.* 90 (1993) 1479–1483.
- [16] L. Luo, T.K. Hensch, L. Ackerman, S. Barbel, L.Y. Jan, Y.N. Jan, Differential effects of the Rac GTPase on Purkinje cell axons and dendritic trunks and spines, *Nature* 379 (1996) 837–840.
- [17] H. Maruta, K. Kohama, *G Proteins, Cytoskeleton, and Cancer*, Landes, New York, 1998.
- [18] T.L. Petit, J.C. LeBoutillier, A. Gregorio, H. Libstug, The pattern of dendritic development in the cerebral cortex of the rat, *Brain Res.* 469 (1988) 209–219.
- [19] J.V. Platko, D.A. Leonard, C.N. Adra, R.J. Shaw, R.A. Cerione, B. Lim, A single residue can modify target-binding affinity and activity of the functional domain of the Rho-subfamily GDP dissociation inhibitors, *Proc. Natl. Acad. Sci. U. S. A.* 92 (1995) 2974–2978.
- [20] S. Rozen, H. Skaletsky, Primer3 on the WWW for general users and for biologist programmers, *Methods Mol. Biol.* 132 (2000) 365–386.
- [21] K. Tanaka, T. Sasaki, Y. Takai, Purification and properties of recombinant Rho-GDP dissociation inhibitor, *Methods Enzymol.* 256 (1995) 41–49.
- [22] A. Tashiro, A. Minden, R. Yuste, Regulation of dendritic spine morphology by the rho family of small GTPases: antagonistic roles of Rac and Rho, *Cereb. Cortex* 10 (2000) 927–938.
- [23] R. Threadgill, K. Bobb, A. Ghosh, Regulation of dendritic growth and remodeling by Rho, Rac, and Cdc42, *Neuron* 19 (1997) 625–634.
- [24] A. Togawa, J. Miyoshi, H. Ishizaki, M. Tanaka, A. Takakura, H. Nishioka, H. Yoshida, T. Doi, A. Mizoguchi, N. Matsuura, Y. Niho, Y. Nishimune, S. Nishikawa, Y. Takai, Progressive impairment of kidneys and reproductive organs in mice lacking Rho GDI α , *Oncogene* 18 (1999) 5373–5380.
- [25] L. Van Aelst, C. D'Souza-Schorey, Rho GTPases and signaling networks, *Genes Dev.* 11 (1997) 2295–2322.